nature physics

LETTERS

PUBLISHED ONLINE: 13 MARCH 2011 | DOI: 10.1038/NPHYS1945

Phase-fluctuating superconductivity in overdoped $La_{2-x}Sr_xCuO_4$

Patrick M. C. Rourke[1], Ioanna Mouzopoulou[1], Xiaofeng Xu[2,3], Christos Panagopoulos[2,4], Yue Wang[5], Baptiste Vignolle[6], Cyril Proust[6], Evgenia V. Kurganova[7], Uli Zeitler[7], Yoichi Tanabe[8], Tadashi Adachi[8], Yoji Koike[8] and Nigel E. Hussey[1]*

In underdoped cuprate superconductors, phase stiffness is low and long-range superconducting order is destroyed readily by thermally generated vortices (and anti-vortices), giving rise to a broad temperature regime above the zero-resistive state in which the superconducting phase is incoherent[1–4]. It has often been suggested that these vortex-like excitations are related to the normal-state pseudogap or some interaction between the pseudogap state and the superconducting state[5–10]. However, to elucidate the precise relationship between the pseudogap and superconductivity, it is important to establish whether this broad phase-fluctuation regime vanishes, along with the pseudogap[11], in the slightly overdoped region of the phase diagram where the superfluid pair density and correlation energy are both maximal[12]. Here we show, by tracking the restoration of the normal-state magnetoresistance in overdoped $La_{2-x}Sr_xCuO_4$, that the phase-fluctuation regime remains broad across the entire superconducting composition range. The universal low phase stiffness is shown to be correlated with a low superfluid density[1], a characteristic of both underdoped and overdoped cuprates[12–14]. The formation of the pseudogap, by inference, is therefore both independent of and distinct from superconductivity.

In underdoped cuprates, an energy gap (pseudogap), of as yet unknown origin, appears in the electronic density of states well before superconductivity develops. The continuous evolution[6] of the pseudogap into the superconducting gap, combined with similarities in their gap magnitudes and symmetries[5], has led to suggestions that the pseudogap is a precursor superconducting state[7–10] characterized by a broad temperature region over which the superconducting order parameter is finite but the phase fluctuates[3,4]. This picture of precursor pairing remains controversial however and is challenged by measurements indicating that the pseudogap itself closes at a critical doping concentration[11], slightly beyond optimal doping, where superconductivity is most robust[12]. As it stands, there have been very few studies to date of the fluctuating superconductivity in overdoped, superconducting cuprates to establish the precise relationship between the pseudogap and phase fluctuation regimes.

To address this, we focus here on the evolution of the upper critical field H_{c2} with temperature, as inferred by measurements of the in-plane resistivity $\rho_{ab}(T,H)$ in pulsed and d.c. magnetic fields. Previous transport studies in cuprates identified $H_{c2}(T)$ with the 'knee' at or near the top of the $\rho_{ab}(T)$ curve or the temperature at which $\rho_{ab}(H)$ attained a certain fraction of the normal-state value[15]. Either technique would lead to a $H_{c2}(T)$ line with a markedly different shape from that determined by the Nernst effect, for example. In this study, we adopt an alternative approach[16,17], using the evolution of the transverse magnetoresistance $\Delta\rho_{ab}(H)(=\rho_{ab}(H)-\rho_{ab}(0)$ with $\mathbf{H} \| c)$ with temperature, field and doping, as our probe. In a single-band metal, $\Delta\rho_{ab}(H)$ varies as H^2 at the lowest fields, this being the lowest-order even response in the longitudinal electrical conductivity to the field-induced Lorentz force[18]. The same behaviour is also observed in optimally and overdoped cuprates well above the phase-fluctuation regime[19]. As the lowest order term in the normal-state magnetoresistance is quadratic, any downward deviation from such quadratic behaviour can only arise from fluctuations associated with some lower resistive state, that is, superconductivity. (In certain underdoped cuprates, the presence of electrons and holes[20] leads to a different form of the magnetoresistance at low fields that has been modelled successfully by assuming the co-existence of two types of carriers[21].) We therefore identify H_{c2} in the optimally and overdoped cuprates as the field at which $\Delta\rho_{ab}(H)$ first recovers its quadratic field dependence. However, as there is no clear thermodynamic phase transition at this particular field scale, in the remainder of this Letter, we shall label it H_2, rather than H_{c2}.

Figure 1a shows representative $\Delta\rho_{ab}(H)/\rho_{ab}(0)$ data at temperatures well above $T_{c0} \sim 32$ K, obtained on a single crystal of $La_{1.79}Sr_{0.21}CuO_4$ (labelled hereafter as LSCO21), which clearly demonstrate the H^2 dependence up to $\mu_0 H = 30$ T. Below $T \sim 60$ K however, as shown in Fig. 1b, the field profile of $\rho_{ab}(H)$ changes and the H^2 dependence is only recovered above a T-dependent field scale (identified by the vertical arrows) that approaches 50 T at low temperatures. Note that this field scale is already large ($\sim$30 T) at $T = T_{c0}$, indicating that the Cooper pair amplitude remains large and robust across the superconducting transition.

The evolution of $H_2(T)$ for LSCO21 is compared with the temperature dependence of the zero-field resistivity $\rho_{ab}(T)$ in Fig. 1c–e. $H_2(T)$ is found to drop monotonically to zero at a temperature $T_2 \sim 60$ K (Fig. 1e) that coincides with a well-defined upturn in $d\rho_{ab}/dT$ (Fig. 1d) marking the onset of superconducting

[1]H. H. Wills Physics Laboratory, University of Bristol, Tyndall Avenue, Bristol, BS8 1TL, UK, [2]Division of Physics and Applied Physics, School of Physical and Mathematical Sciences, Nanyang Technological University, 637371 Singapore, Singapore, [3]Department of Physics, Hangzhou Normal University, Hangzhou 310036, China, [4]Department of Physics, University of Crete and FORTH, 71003 Heraklion, Greece, [5]State Key Laboratory for Mesoscopic Physics and School of Physics, Peking University, Beijing 100871, China, [6]Laboratoire National des Champs Magnetiques Intenses (CNRS, INSA, UJF, UPS), Toulouse 31400, France, [7]High Field Magnet Laboratory, Institute for Molecules and Materials, Radboud University Nijmegen, Toernooiveld 7, 6525 ED Nijmegen, The Netherlands, [8]Department of Applied Physics, Graduate School of Engineering, Tohoku University, 6-6-05 Aoba, Aramaki, Aoba-ku, Sendai 980-8579, Japan. *e-mail: n.e.hussey@bristol.ac.uk.

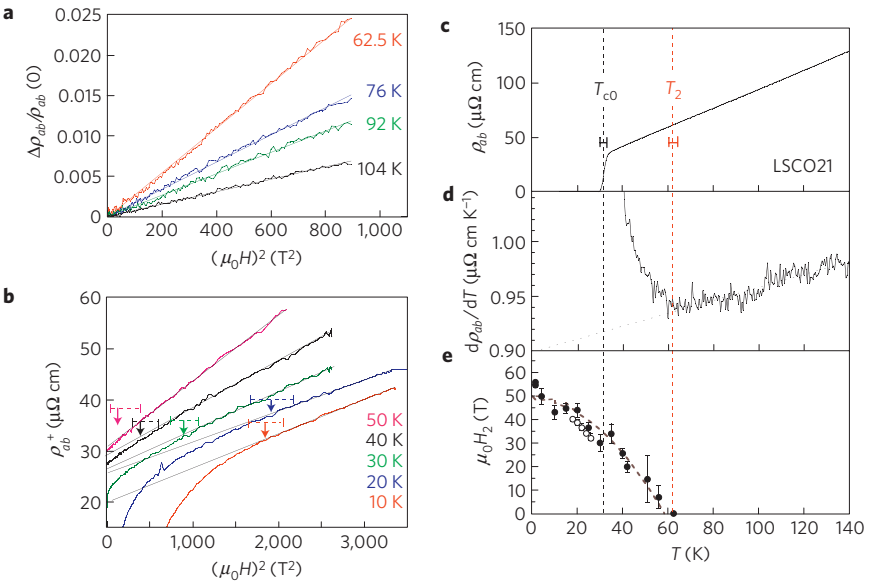

Figure 1 | Fluctuating superconductivity in $La_{1.79}Sr_{0.21}CuO_4$ (LSCO21). a,b, Transverse in-plane magnetoresistance $\Delta\rho_{ab}(H)$ (**H** ∥ *c*) plotted versus H^2 both above **a** and below **b** the onset temperature for fluctuating superconductivity T_2. In **a**, the data are normalized to $\rho_{ab}(0)$, the zero-field resistivity value. In **b**, the superscript '+' indicates that the $\rho_{ab}(H)$ have been offset for clarity. The solid lines in **a** and **b** highlight the region of H^2 magnetoresistance (MR), and the solid arrows and the dashed horizontal error bars in **b** indicate respectively the upper field H_2 and its associated uncertainty (see Error bars section) at which the normal-state (H^2) MR is recovered. **c**, Zero-field resistivity $\rho_{ab}(T)$ curve for LSCO21. The superconducting transition temperature T_{c0} is defined by the midpoint of the superconducting transition. **d**, Temperature derivative $d\rho_{ab}/dT$ of the same resistivity curve shown in **c**. Here, T_2 is indicated by the minimum in $d\rho_{ab}/dT$. The dotted line is a guide to the eye. **e**, Solid circles: temperature dependence of H_2 as determined by the restoration of the normal-state MR. Open circles: $H_2(T)$ as determined by Nernst effect measurements on LSCO20 (ref. 22). The thick dashed line is a fit to the two-fluid expression $H_2(T) = H_2(0)(1-(T/T_2)^2)$ with $H_2(0) = 48.5$ T and $T_2 = 58.5$ K. The vertical dashed line highlights the coincidence of T_2 in **d** and **e**. The horizontal error bars in **c** indicate our uncertainty in the two temperature scales T_{c0} and T_2.

fluctuations. Although the upturn in $d\rho_{ab}/dT$ is significant (it increases by around 10% on cooling from 60 to 40 K), the absolute change in $\rho_{ab}(T)$ from its extrapolated normal-state behaviour is extremely small (of order 1 μΩ cm), despite the fact that over the same temperature interval H_2 has increased to around 30 T.

In Fig. 1e, we also compare our estimates for H_2 with those determined from earlier Nernst measurements (over a narrower temperature range) on a crystal of similar doping (LSCO20; ref. 22). Reasonable agreement is found between the two approaches, although if anything, it would seem that the Nernst effect tends to underestimate H_2, presumably owing to the fact that such estimates rely on a linear extrapolation of a finite Nernst signal e_y to zero[22]. Note that $H_2(T)$ obtained in either case follows approximately the simple two-fluid expression, $H_2(T) = H_2(0)(1-(T/T_2)^2)$. The phase diagram thus obtained is highly reminiscent of the temperature–field profile expected for a two-dimensional Berezinsky–Kosterlitz–Thouless (BKT) transition[23], as is the fluctuation conductivity described in Supplementary Fig. S1. Here T_{c0} corresponds to the temperature at which long-range phase coherence is destroyed by thermally generated vortex–antivortex pairs, whereas T_2 represents the temperature beyond which the pairing amplitude is zero.

Figure 2a shows $H_2(T)$ for a number of overdoped LSCO crystals with Sr concentrations ranging between 0.21 and 0.26. (The analysis presented in Fig. 1 for LSCO21 is repeated in Supplementary Figs S2–S4 for LSCO23, LSCO24 and LSCO26 respectively.) One surprising feature of Fig. 2a is that whereas the absolute value of $H_2(0)$ decreases with increasing doping, the onset temperature T_2 remains high, and even rises slightly as x increases from 0.21 to 0.24. Beyond $x = 0.24$, both $H_2(0)$ and T_2 seem to collapse as the edge of the superconducting dome is approached. The evolution of both $H_2(0)$ and T_2 across the phase diagram are summarized in Fig. 2b and c respectively. In Fig. 2b, values of $H_2(0)$ for lower hole concentrations (that is, below $x = 0.21$) are extracted from published Nernst results[24] and from low-temperature specific heat[25]. There is clear agreement between the different experimental techniques. The suppression of $H_2(0)$ with overdoping reflects the overall reduction in the superconducting pairing strength as the system is doped further away from the parent Mott insulator.

The contrasting doping dependencies of T_2 and the pseudogap temperature T^* for LSCO are highlighted in Fig. 2c. Here T^* is defined as the temperature below which $\rho_{ab}(T)$ first deviates from its high temperature T-linear behaviour. For $x < 0.19$, both $T^*(x)$ and $T_2(x)$ decrease monotonically with increasing x and, indeed, follow an approximate scaling relation with $T^* \sim 2T_2$. Such a good correspondence has contributed considerably to the widespread association of the two temperature scales to the same physical phenomenon, namely precursor superconductivity. However, whereas $T_2(x)$ remains roughly constant between $x = 0.19$ and $x = 0.24$, T^* becomes difficult to track as it dips below T_2. The precise location of the critical hole doping concentration p_{crit} at which the cuprate pseudogap closes has long been a controversial issue, although there is now a large body of evidence from bulk physical measurements that T^* and the pseudogap energy scale do not extend into the heavily overdoped region of the phase diagram but rather collapse at a well-defined critical concentration around $p_{crit} = 0.19 \pm 0.01$, irrespective of the cuprate system[11]. Beyond $x = 0.19$, a new temperature scale T_{coh} appears in the phase diagram, again associated with the recovery of T-linear resistivity at high temperatures[26], but this time corresponding to the loss of quasiparticle coherence, predominantly for states with momenta near the zone boundary[27]. The crucial distinction between T^* and T_{coh} in LSCO is the doping dependence; whereas T^* decreases with increasing x, T_{coh} shows the opposite trend.

To parameterize the extent of the fluctuation regime, we plot in Fig. 2d the ratio T_2/T_{c0} versus hole content p (solid red squares).

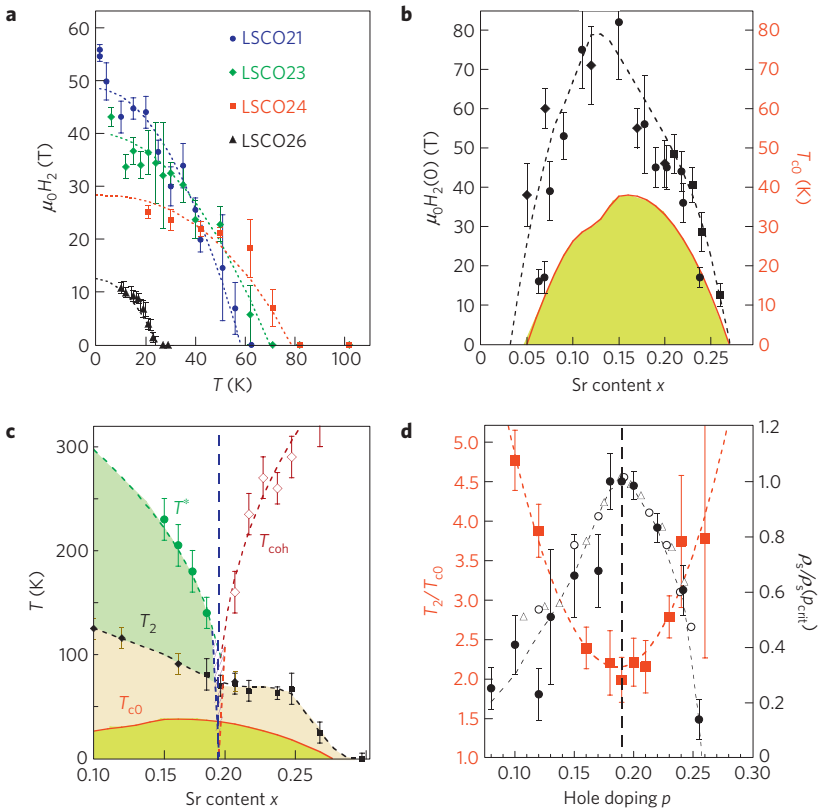

Figure 2 | Evolution of the upper field $H_2(T)$ and the phase diagram for overdoped LSCO. a, Temperature dependence of the upper field $H_2(T)$ for LSCO21 (solid blue circles), LSCO23 (solid green diamonds), LSCO24 (solid red squares) and LSCO26 (solid black triangles). The dashed lines are fits to the expression $H_2(T) = H_2(0)\,(1-(T/T_2)^2)$. **b**, The doping dependence of H_2 (0) as determined by the Nernst effect (solid diamonds, ref. 24), the coefficient of the $H^{0.5}$ field-dependence of the low temperature electronic specific heat (solid circles, ref. 25) and our magnetoresistance measurements (solid squares). The solid red curve denotes the doping dependence of the superconducting transition temperature $T_{c0}(x)$. **c**, Temperature versus doping phase diagram of LSCO as extracted from the temperature derivative of $\rho_{ab}(T)$ (ref. 26). The labels T_{c0}, T_2, T^*, T_{coh} represent respectively the zero-field superconducting transition temperature, the onset temperature for short-lived vortex excitations, the opening of the pseudogap and the onset of anti-nodal quasiparticle incoherence[27]. For the purposes of this study, T^* and T_{coh} are identified with the downturns in $d\rho_{ab}/dT$ for $x < 0.19$ and $x > 0.19$ respectively[26]. The solid diamonds correspond to T_2 values obtained from Nernst measurements on LSCO (ref. 24). The dashed lines are all guides to the eye. The hatched region reflects current uncertainty in the behaviour of T^* and T_{coh} around $p_{crit} = 0.19$. **d**, Ratio of T_2/T_{c0} versus hole content p (solid squares) superimposed on a plot of the normalized superfluid density $\rho_s/\rho_s(p_{crit})$ for LSCO (solid circles, $p_{crit} = 0.19 \pm 0.01$), Ca-doped $YBa_2Cu_3O_{6+\delta}$ (open circles) and $Tl_{0.5-y}Pb_{0.5+y}Sr_2Ca_{1-x}Y_xCu_2O_7$ (open triangles)[12], illustrating the anti-correlation between ρ_s and the extent of the fluctuation regime. For determination of $\rho_s/\rho_s(p_{crit})$ for LSCO, and its associated error, please refer to Supplementary Table S1. For a description of all the associated errors, please refer to the Error bars section.

Despite the non-monotonic and asymmetric form of $T_2(x)$ in Fig. 2c, the ratio T_2/T_{c0} turns out to be surprisingly symmetrical, with a minimum at $x = p_{crit}$. There is no obvious reason for amplitude fluctuations to follow such a trend. According to the original argument of Emery and Kivelson[1], phase stiffness is determined predominantly by the superfluid density ρ_s; the smaller the ρ_s, the weaker the screening and the larger the region over which classical (thermal) phase fluctuations are important. In underdoped cuprates, ρ_s is found to decrease monotonically with T_{c0} (ref. 28), indicating that the condensate density drops as p is reduced. Significantly, in overdoped cuprates, ρ_s also falls away as T_{c0} decreases[13,14].

The solid circles in Fig. 2d correspond to estimates of the normalized superfluid density $\rho_s/\rho_s(p_{crit})$ for LSCO (see Supplementary Table S1 for a description of how $\rho_s/\rho_s(p_{crit})$ is determined at each p value). Also included in Fig. 2d for comparison are $\rho_s/\rho_s(p_{crit})$ values obtained for Ca-doped $YBa_2Cu_3O_{6+\delta}$ (open circles) and $Tl_{0.5-y}Pb_{0.5+y}Sr_2Ca_{1-x}Y_xCu_2O_7$ (open triangles)[12]. The clear anti-correlation between T_2/T_{c0} and $\rho_s(p)$ supports the Emery–Kivelson picture[1] and provides firm evidence that the temperature interval $T_{c0} \leq T \leq T_2$ in overdoped cuprates is characterized by the same phase fluctuations that appear on the underdoped side. In underdoped cuprates, the reduction in the superfluid density (that subsequently enhances the phase fluctuation regime) is attributed to the formation of the normal-state pseudogap, which progressively removes spectral weight that is never recovered on entering the full Meissner state. In overdoped cuprates, the strong suppression of ρ_s has been attributed both to phase separation[13] and to pair-breaking[14]. Whatever its origin, the observed persistence of an extended fluctuation regime beyond $x = p_{crit}$ in LSCO reveals that low phase rigidity in high-T_c cuprates does not require the presence of a pseudogap in the normal-state excitation spectrum and that the pseudogap itself is not a precondition for the development of an extended region of phase-fluctuating superconductivity.

Detailed Nernst data on irradiated samples of underdoped and optimally doped $YBa_2Cu_3O_{7-\delta}$ have shown that although T_{c0} is strongly suppressed with increasing disorder, T_2 is much less affected[29]. In accord with the anti-correlation reported here between T_2/T_{c0} and ρ_s, one can now interpret the expansion of the fluctuation regime in irradiated $YBa_2Cu_3O_{7-\delta}$ as a direct consequence of the strong disorder-induced suppression of the superfluid density[12], which ultimately enhances the role of phase fluctuations.

The strong disorder inherent in LSCO presumably plays a key role in amplifying T_2/T_{c0} here too. The relation between T_{c0} and T_2 is explored in more detail in the Supplementary Information.

Finally, the observation of an expanded phase-fluctuation regime in overdoped cuprates may help to explain why certain spectroscopic probes, such as angle-resolved photoemission, tend to advocate scenarios in which T^* tracks the superconducting dome on the overdoped side, rather than vanishing inside it. This difference could arise from the difficulty in distinguishing spectroscopically between the loss of states due to the opening of the normal-state pseudogap and the loss of states due to superconducting fluctuations. Note that in LSCO, T^* and T_2 are easily distinguished by in-plane resistivity data as they are identified respectively by a downturn and an upturn in $d\rho_{ab}/dT$ (ref. 26). The ubiquity of phase-fluctuating superconductivity and the coincidence between T_2, as determined by $d\rho_{ab}/dT$, and the vanishing of $H_2(T)$, as determined by the high-field magnetoresistance, imply that one might now be able to identify the phase fluctuation regime in any cuprate system (at or beyond optimal doping) simply by taking the first (or second) derivative of the zero-field resistivity curve. Indeed, excellent agreement is already noted between the fluctuation onset temperatures determined by the Nernst effect and magnetization in LSCO, $Bi_2Sr_{2-y}La_yCuO_6$ and optimally doped $YBa_2Cu_3O_7$ and the corresponding T_2 values obtained from $d^2\rho_{ab}/dT^2$ analysis of Ando and co-workers[30]. Such agreement suggests that it should be relatively straightforward to generalize these findings to other new or existing cuprate families.

Methods

Single crystals of $La_{2-x}Sr_xCuO_4$ (LSCO) were grown using a travelling-solvent-floating-zone technique. The actual doping $x(=p)$ of each crystal was estimated from its T_c using the empirical relation $T_{c0} = T_c^{opt}(1-82.6(p-0.16)^2)$ (ref. 31). The in-plane resistivity ρ_{ab} was measured using a conventional four-probe a.c. lock-in detection technique in a superconducting magnet at the University of Bristol, in steady magnetic fields up to 33 T at the High Magnetic Field Laboratory (HMFL) in Nijmegen, and in pulsed magnetic fields up to 60 T at the LNMCI-T in Toulouse. In all reported measurements, the field was applied along the c-axis.

Error bars. The error bars in Figs 1e and 2a (and subsequently in Fig. 2b) reflect our uncertainty in the determination of $H_2(T)$ from the individual magnetoresistance curves. More explicitly, we fit the highest-field data, well above H_2, to a quadratic field dependence and determine the standard deviation σ from the fit. We then identify H_2 (and its associated uncertainty) with the point at which the data deviate from the extrapolated high-field fit by more than 3σ ($\pm 1\sigma$). The error bars in the Nernst- and specific-heat-derived points are as quoted in the corresponding references. In Fig. 2c, the error bars for T^*, T_{coh} and T_2 represent compound errors due to uncertainty in determining the various onset temperatures and the spread in values as measured on samples of the same x. The T^*, T_{coh} and T_2 values quoted are averages of measurements taken on at least three different samples for each doping concentration. In Fig. 2d, the error bars associated with T_2/T_{c0} are again compound errors—the large error bars for LSCO26 reflect for the most part our uncertainty in T_{c0}, the superconducting transition of which is invariably broader as it resides at the edge of the superconducting dome where dT_{c0}/dx is the steepest. The error bars for $\rho_s/\rho_s(p_{crit})$ represent the standard deviation in the spread of values as listed in Supplementary Table S1.

Received 4 October 2010; accepted 7 February 2011; published online 13 March 2011

References

1. Emery, V. J. & Kivelson, S. A. Importance of phase fluctuations in superconductors with small superfluid density. *Nature* **374,** 434–437 (1995).
2. Corson, J., Mallozzi, R., Orenstein, J., Eckstein, J. N. & Bozovic, I. Vanishing of phase coherence in underdoped $Bi_2Sr_2CaCu_2O_{8+\delta}$. *Nature* **398,** 221–223 (1999).
3. Xu, Z. A., Ong, N. P., Wang, Y., Kakeshita, T. & Uchida, S. Vortex-like excitations and the onset of superconducting phase fluctuation in underdoped $La_{2-x}Sr_xCuO_4$. *Nature* **406,** 486–488 (2000).
4. Wang, Y. *et al.* Field-enhanced diamagnetism in the pseudogap state of the cuprate $Bi_2Sr_2CaCu_2O_{8+\delta}$ superconductor in an intense magnetic field. *Phys. Rev. Lett.* **95,** 247002 (2005).
5. Ding, H. *et al.* Spectroscopic evidence for a pseudogap in the normal state of underdoped high-T_c superconductors. *Nature* **382,** 51–54 (1996).
6. Loeser, A. G. *et al.* Temperature and doping dependence of the Bi–Sr–Ca–Cu–O electronic structure and fluctuation effects. *Phys. Rev. B* **56,** 14185–14189 (1997).
7. Nagaosa, N. & Lee, P. A. Ginzburg–Landau theory of the spin-charge-separated system. *Phys. Rev. B* **45,** 966–970 (1992).
8. Randeria, M., Trivedi, N., Moreo, A. & Scalettar, R. T. Pairing and spin gap in the normal state of short coherence length superconductors. *Phys. Rev. Lett.* **69,** 2001–2004 (1992).
9. Perali, A. *et al.* Two-gap model for underdoped cuprate superconductors. *Phys. Rev. B* **62,** R9295–R9298 (2000).
10. Lee, J. *et al.* Spectroscopic fingerprint of phase-incoherent superconductivity in the underdoped $Bi_2Sr_2CaCu_2O_{8+\delta}$. *Science* **325,** 1099–1103 (2009).
11. Tallon, J. L. & Loram, J. W. The doping dependence of T^*—what is the real high-T_c phase diagram? *Physica* **349C,** 53–68 (2001).
12. Bernhard, C. *et al.* Anomalous peak in the superconducting condensate density of cuprate high-T_c superconductors at a unique doping state. *Phys. Rev. Lett.* **86,** 1614–1617 (2001).
13. Uemura, Y. J. *et al.* Magnetic-field penetration depth in $Tl_2Ba_2CuO_{6+\delta}$ in the overdoped regime. *Nature* **364,** 605–607 (1993).
14. Niedermayer, Ch. *et al.* Muon spin rotation study of the correlation between T_c and n_s/m^* in overdoped $Tl_2Ba_2CuO_{6+\delta}$. *Phys. Rev. Lett.* **71,** 1764–1767 (1993).
15. Ando, Y. *et al.* Resistive upper critical fields and irreversibility lines of optimally doped high-T_c cuprates. *Phys. Rev. B* **60,** 12475–12479 (1999).
16. Rullier-Albenque, F. *et al.* Total suppression of superconductivity by high magnetic fields in $YBa_2Cu_3O_{6.6}$. *Phys. Rev. Lett.* **99,** 027003 (2007).
17. Cooper, R. A. *et al.* Anomalous criticality in the electrical resistivity of $La_{2-x}Sr_xCuO_4$. *Science* **323,** 603–607 (2009).
18. Pippard, A. B. *Magnetoresistance in Metals* (Cambridge Univ. Press, 1989).
19. Kimura, T. *et al.* In-plane and out-of-plane magnetoresistance in $La_{2-x}Sr_xCuO_4$ single crystals. *Phys. Rev. B* **53,** 8733–8742 (1996).
20. LeBoeuf, D. *et al.* Electron pockets in the Fermi surface of hole-doped high-T_c superconductors. *Nature* **450,** 533–536 (2007).
21. Rourke, P. M. C. *et al.* Fermi-surface reconstruction and two-carrier model for the Hall effect in $YBa_2Cu_4O_8$. *Phys. Rev. B* **82,** 020514(R) (2010).
22. Wang, Y. *et al.* High field phase diagram of cuprates derived from the Nernst effect. *Phys. Rev. Lett.* **88,** 257003 (2002).
23. Doniach, S. & Huberman, B. A. Topological excitations in two-dimensional superconductors. *Phys. Rev. Lett.* **42,** 1169–1172 (1979).
24. Wang, Y., Li, L. & Ong, N. P. Nernst effect in high-T_c superconductors. *Phys. Rev. B* **73,** 024510 (2006).
25. Wang, Y. & Wen, H. H. Doping dependence of the upper critical field in $La_{2-x}Sr_xCuO_4$ from specific heat. *Europhys. Lett.* **81,** 57007 (2008).
26. Hussey, N. E. *et al.* Dichotomy in the T-linear resistivity in high-T_c cuprates. Preprint at http://arxiv.org/abs/0912.2001v1.
27. Kaminski, A. *et al.* Crossover from coherent to incoherent electronic excitations in the normal state of $Bi_2Sr_2CaCu_2O_{8+\delta}$. *Phys. Rev. Lett.* **90,** 207003 (2003).
28. Uemura, Y. J. *et al.* Universal correlations between T_c and n_s/m^* (carrier density over effective mass) in high-T_c cuprate superconductors. *Phys. Rev. Lett.* **62,** 2317–2320 (1989).
29. Rullier-Albenque, F. *et al.* Nernst effect and disorder in the normal state of high-T_c cuprates. *Phys. Rev. Lett.* **96,** 067002 (2006).
30. Ando, Y., Komiya, S., Segawa, K., Ono, S. & Kurita, Y. Electronic phase diagram of high-T_c cuprate superconductors from a mapping of the in-plane resistivity curvature. *Phys. Rev. Lett.* **93,** 267001 (2004).
31. Tallon, J. L. *et al.* Generic superconducting phase behaviour in high-T_c cuprates: T_c variation with hole concentration in $YBa_2Cu_3O_{7-\delta}$. *Phys. Rev. B* **51,** 12911–12914 (1995).

Acknowledgements

The authors would like to acknowledge R. A. Cooper for experimental assistance, S. M. Hayden and O. J. Lipscombe for providing us with the LSCO23 crystals, and J. P. Annett, A. Carrington, B. Gyorffy, R. H. McKenzie, T. Senthil, N. Shannon, T. Timusk, Y. J. Uemura and J. A. Wilson for fruitful discussions. This work was supported by EPSRC (UK), MEXT-CT-2006-039047, EURYI, the National Research Foundation, Singapore and EuroMagNET under EU contract 228043. N.E.H. acknowledges a Royal Society Wolfson Research Merit Award.

Author contributions

All authors made critical comments on the manuscript. Y.T., T.A. and Y.K. synthesized the samples. P.M.C.R., I.M., X.X., Y.W., B.V., C.P., E.V.K., U.Z. and N.E.H. carried out the transport measurements. P.M.C.R., I.M. and N.E.H. analysed and interpreted the transport data.

Additional information

The authors declare no competing financial interests. Supplementary information accompanies this paper on www.nature.com/naturephysics. Reprints and permissions information is available online at http://npg.nature.com/reprintsandpermissions. Correspondence and requests for materials should be addressed to N.E.H.